Journal of Photochemistry & Photobiology, A: Chemistry 411 (2021) 113205

Contents lists available at ScienceDirect

Journal of Photochemistry & Photobiology, A: Chemistry

journal homepage: www.elsevier.com/locate/jphotochem

Treatment of ethylmercury chloride by heterogeneous photocatalysis with TiO_2

Emmanuel M. de la Fournière [a], Jorge M. Meichtry [a,b], Eduardo A. Gautier [a], Ana G. Leyva [a], Marta I. Litter [c,*]

[a] Comisión Nacional de Energía Atómica, Av. Gral. Paz 1499, 1650, San Martín, Prov. de Buenos Aires, Argentina
[b] Centro de Tecnologías Químicas, Facultad Regional Buenos Aires, Universidad Tecnológica Nacional, Medrano 951, 1425, Buenos Aires, Argentina
[c] Instituto de Investigación e Ingeniería Ambiental –IIIA, UNSAM, CONICET, 3iA, Universidad de San Martín, Campus Miguelete, 25 de Mayo y Francia, 1650, San Martín, Prov. de Buenos Aires, Argentina

ARTICLE INFO

Keywords:
Heterogeneous photocatalysis
Ethylmercury chloride
Titanium dioxide

ABSTRACT

Ethylmercury chloride (C_2H_5HgCl) was treated by UV/TiO_2 photocatalysis in the presence of O_2 and under N_2 at pH 4.2. No report exists on $C_2H_5Hg^+$ degradation by heterogeneous photocatalysis. The adsorption of $C_2H_5Hg^+$ over TiO_2 (no irradiation) was studied and fitted to the Freundlich isotherm. The photocatalytic evolution of $C_2H_5Hg^+$ was adjusted to a two parameter Langmuir-Hinshelwood model, modified to include a third parameter attributed to the deactivation caused by the deposition of Hg(0). Hg(II) in solution, Hg(0) and Hg_2Cl_2 (detected only under N_2) were the products of the photocatalytic degradation; the organic moiety was degraded but no organic by-product could be detected. Experiments in the absence of O_2 showed a higher conversion rate, indicating that $C_2H_5Hg^+$ is removed both by oxidative and reductive pathways, being this last step partially inhibited by O_2. A degradation mechanism considering both oxidative and reductive one-electron transfer steps is proposed.

1. Introduction

Mercury is a hazardous and persistent contaminant, which can cause neurological disorders, birth defects and immune system dysfunction, among other health effects in humans; polluted waters are the main exposure source [1,2]. Mercury compounds are extremely hazardous and are known to contaminate water coming from anthropogenic and natural processes [3–5]. Both inorganic and organic mercury are cumulatively toxic and the latter form is known to be more dangerous, mainly the alkylated derivatives [6]. The most important anthropogenic sources of mercury pollution in aquatic systems are urban discharges, agricultural materials, mining and discharges from pyrometallurgical processes and chlor-alkali industry. Atmospheric mercury deposition coming mainly from coal combustion is also a major contributor to aquatic pollution [7]. Despite it has not been employed as frequently as other organomercurial species like methylmercury (CH_3Hg^+), phenylmercury ($C_6H_5Hg^+$) or thiomersal (mercury((o-carboxyphenyl)thio) ethyl sodium), ethylmercury ($C_2H_5Hg^+$) has been used as a pesticide, mainly as its chloride, urea and phosphate salts and methoxydes. Besides, $C_2H_5Hg^+$ can be produced in natural aquatic systems by photoalkylation of Hg^{2+} in the presence of ketones, aldehydes and low molecular weight organic acids under UV irradiation [8], or by microorganisms during the metabolism of inorganic mercury [9,10]; it is also a metabolite of thiomersal, a preservative used in vaccines [11]. The lack of information related to $C_2H_5Hg^+$ could be attributed to previous analytical limitations at trace level; i.e., $CH_3CH_2Hg^+$ was considered a misidentification of CH_3SHg^+ [12]. Nowadays, its identification and verification is unmistakable [13].

Mercury removal can be carried out efficiently by heterogeneous photocatalysis over TiO_2 with several advantages compared with other technologies like precipitation as sulfide, ion exchange, adsorption, coagulation and chemical reduction [14] because it does not require the use of expensive chemicals and only near UV light is needed, allowing the use of free solar light [5,15–21]. As very well known, the photocatalytic process begins by the semiconductor excitation with light of enough energy to promote an electron from the valence band (VB) to the conduction band (CB) [15,17–21 and references therein]. A sequence of reactions occurs, the main ones depicted in Section A1 of Appendix A.

* Corresponding author.
E-mail address: marta.litter@gmail.com (M.I. Litter).

https://doi.org/10.1016/j.jphotochem.2021.113205
Received 5 October 2020; Received in revised form 5 February 2021; Accepted 8 February 2021
Available online 13 February 2021

Supplementary data (SD).

We have postulated that the photocatalytic transformation of ionic metals occurs through successive one-electron transfer steps, if they are thermodynamically allowed (Eqs. (A8)-(A16)) [18,19]. This fact is generally not taken into account by most photocatalytic researchers, despite multielectronic processes are not feasible at the low light intensities usually employed in photocatalysis, and no proof of these processes in semiconductor photocatalytic systems has been reported [22].

In the case of the UV/TiO_2 photocatalytic reaction of inorganic Hg (II) in aqueous solutions [14,23–27], conversions have been found to be dependent on the initial conditions (pH, presence or absence of O_2), counterion of Hg(II) ($Hg(NO_3)_2$, $Hg(ClO_4)_2$ or $HgCl_2$), and concentration of mercuric salt. Hg(0), HgO (at high pH) or Hg_2Cl_2 (when chloride was present) are the most important products; calomel is exclusively obtained under acid conditions [25]. Although deposition of solid mercury species over the TiO_2 surface poisons the photocatalyst, reduces the effectiveness of light absorption and decreases the activity [23], being a disadvantage of the method, it can lead to recover of mercury from the solution.

If successive monoelectronic steps are assumed for the photocatalytic reduction of Hg(II) to Hg(0) [14,19], the first step should be the transformation of Hg(II) to Hg(I) followed by reduction up to Hg(0) according to Eqs. (1) and (2). Mononuclear Hg(I) is very unstable and, if formed, it would be rapidly transformed to the binuclear form, Hg_2^{2+} (Eq. (3)) or would later disproportionate to Hg(0) and Hg(II), which further react to form Hg_2^{2+} (Eq.(4)) [21 and refs. therein]:

$$Hg(II) + e^-_{CB} \rightarrow Hg(I) \quad (1)$$

$$Hg(I) + e^-_{CB} \rightarrow Hg(0) \quad (2)$$

$$2\ Hg(I) \rightarrow Hg_2^{2+} \quad (3)$$

$$Hg_2^{2+} \rightleftarrows Hg(0) + Hg(II) \quad (4)$$

If Cl^- is present, calomel is formed:

$$Hg_2^{2+} + 2\ Cl^- \rightarrow Hg_2Cl_2 \quad (5)$$

As the redox potential for the direct reduction of non-complexed Hg (II) to Hg(I) was estimated to be lower than −2.0 V [21], the direct reduction by the TiO_2 e^-_{CB} would not be feasible; on the other hand, when Cl^- is present and the main Hg(II) species is $HgCl_2$, the direct reduction of $HgCl_2$ to HgCl might take place ($E°_{HgCl2/HgCl} = -0.47$ V at $[Cl^-] = 0.05$ M) [21 and references therein]. The formation of Hg(I) as Hg_2Cl_2 has been reported as stable final product when the reaction started from $HgCl_2$, while salts of other anions produced Hg(0) [18,20,21].

Hg_2Cl_2 can be generated also by reoxidation of Hg(0) by $Cl^•$ radicals, a rather powerful oxidative species, formed by reaction of h^+_{VB} with Cl^- ions, if present [14,21]:

$$Cl^- + h^+_{VB} \rightarrow Cl^• \quad (6)$$

$$2\ Cl^• + 2\ Hg(0) \rightarrow Hg_2Cl_2 \quad (7)$$

Actually, the photocatalytic reduction of Hg(II) nitrate and perchlorate was only important at high pH values, with rather low conversions at pH 3–6 (e.g., [14,23,28,29]). Under acid conditions, reduction of Hg(II) is slow, and reoxidation of deposited Hg(0) on the TiO_2 surface by $h^+_{VB}/HO^•$ takes place (Eq. (8)).

$$Hg(0/I) + h^+_{VB}/HO^• \rightarrow Hg(I/II) \quad (8)$$

Species more oxidizable than water (Eq. (A14), such as methanol, EDTA, citric, oxalic, salicylic, formic acids, etc., act as electron donors, leading to mercury reduction synergically helped by indirect reduction (Eqs. (A15) and (A16)) [24,25,30], and sacrificial agents that consume holes greatly enhance the deposition of the metal.

Inorganic forms of heavy metals (i.e. the ionic species) cannot be removed from water by photocatalytic methods in the presence of oxygen. The electrons photogenerated in the catalyst are accepted by oxygen to yield $O_2^{•-}$ (Eq. (9)).

$$O_2 + e^-_{CB} \rightarrow O_2^{•-} \quad (9)$$

In the absence of O_2, electrons can be accepted by heavy metal cations resulting in the deposition of the metal on the surface of the catalyst or in the transformation of a less toxic species (Eq. (A8)), as the transformation of Cr(VI) to Cr(III) [20,31]. For the case of mercury, O_2 inhibits mercury reduction in all cases [14,32] because this species competes with Hg(II) species for TiO_2 CB electrons (Eqs. (1) and (2)). Oxygen is also an efficient electron acceptor, but for practical applications, deoxygenation of polluted water is prohibitively expensive. For this reason, it is essential to develop cheap techniques that work effectively even in oxygenated solutions. It is important to say that inhibition by O_2 was not observed at basic pH.

The presence of organic molecules increases the mercury removal efficiency, particularly at acid pH values [25,30,33,34], preventing the reoxidation of Hg(0) by efficiently trapping $h^+_{VB}/HO^•$ (Eq. (A14)); also, the formation of highly reducing radicals (Eq. (A15)) helps the reaction.

Tennakone and Ketipearachchi found that oxidative TiO_2 photodegradation of the complex of Hg^{2+} with citrate led to metallic mercury deposited on TiO_2. The reaction was sufficiently sensitive to sunlight, and ca. 20 ppm Hg^{2+} were removed in around 30 min exposure. For practical applications, the authors confined TiO_2 in a transparent dialysis bag immersed in the solution to facilitate the disposal of extracted mercury [35].

Only few reports exist regarding the treatment of organic (mainly alkyl) mercury compounds in aqueous solution: CH_3Hg^+ degradation by heterogeneous photocatalysis has been studied by Serpone et al. [29] and by Miranda et al. [34].

Serpone et al. [29] studied CH_3HgCl removal (3.7×10^{-4} M, 2 g L^{-1} TiO_2 air equilibrated suspensions, pH 6.36) irradiated by AMI simulated sunlight ($\lambda > 310$ nm); a 75 % removal after 60 min has been found. According to the authors, in this case, removal was mostly due to adsorption than to photoreduction. Elemental mercury, deposited on TiO_2 particles as a gray powder, was obtained; the authors propose methane formation, according to global Eq. (10), although the presence of methane was not experimentally proved:

$$CH_3HgCl + H_2O\ (h\nu/TiO_2) \rightarrow 1/2\ O_2 + H^+ + Cl^- + Hg(0) + CH_4 \quad (10)$$

Addition of 20 % v/v methanol to the system led to total elimination of CH_3Hg^+ in ca. 30 min irradiation. The authors proposed for the first time photocatalytic reductive pathways for CH_3Hg^+ removal, through a direct photoreduction process by CB electrons, where the one-electron reduction yields first the $CH_3Hg^•$ radical (Eq. (11)), followed by $CH_3Hg^•$ recombination (Eq. (12)) or reduction by another e^-_{CB} (Eq. (13)):

$$CH_3Hg^+ + e^-_{CB} \rightarrow CH_3Hg^• \quad (11)$$

$$2\ CH_3Hg^• \rightarrow (CH_3)_2Hg + Hg(0) \quad (12)$$

$$CH_3Hg^• + H^+ + e^-_{CB} \rightarrow CH_4 + Hg(0) \quad (13)$$

Miranda et al. [34] reported TiO_2-photocatalytic methylmercury removal in the presence of nitrogen or oxygen. Under N_2, using low amounts of catalyst (0.15 g L^{-1}) and pH 11, more than 95 % of removal was achieved after 2 min irradiation. Destruction of the organic moiety to CH_3OH and no gaseous products were observed, and the reaction proceeded by forming water soluble compounds, such as methanol or more oxidized compounds, with Hg(0) formation (Eqs. (14)–(16)):

$$CH_3HgCl + 2\ HO^• \rightarrow CH_3OH + Hg^{2+} + Cl^- + OH^- \quad (14)$$

$$CH_3OH + h^+_{VB} \rightarrow H_2CO \rightarrow HCO_2H \quad (15)$$

$$Hg^{2+} + 2\ e^-_{CB} \rightarrow Hg(0) \quad (16)$$

In saturated O_2 solutions, the reaction slowed down due to competition between oxygen and Hg(II) for CB electrons; the main reaction products were CH_4 (minor amounts), CO and CO_2. Methanol was identified as a reaction intermediate in solution. Hg(0) was found as a final reduction product also in the gas phase. The authors proposed that CH_3Hg^+ is oxidized to methanol by h^+_{VB}, $HO^\bullet$, $HOO^\bullet$, or $O_2^{\bullet -}$, while Hg^{2+} is then reduced to Hg(0) by e^-_{CB}, in contrast with the reductive mechanism proposed by Serpone et al. [29] for CH_3Hg^+.

Our group investigated the photocatalytic removal of phenylmercury chloride (PMC) and phenylmercury acetate (PMA) over P25 [36], a study completed by Miranda et al. [37]. For PMC and PMA, our group obtained a high mercury conversion under UV/TiO_2 irradiation [36] with partial mineralization of the organic portion of the mercurial compound. Mercury species were detected in solution as $C_6H_5Hg^+$ and free Hg^{2+}. The simultaneous deposit of metallic Hg (when starting from PMA) or mixtures of Hg(0) and Hg_2Cl_2 (when starting from PMC) was observed. For PMA, reaction was faster at pH 11 with formation of Hg and HgO mixtures. The fact that calomel was found as a deposit when starting from PMC under N_2 suggests that the mechanism of Hg(II) transformation proceeds, as in the other cases, through successive one-electron transfer reactions passing through a mercurous form. A mixed oxidative and reductive mechanism, where phenylmercury was degraded according to Eq. (17), followed by Hg(II) monoelectronic reduction (Eqs. (A11) and (A12)), was proposed. The anodic pathways can continue through Eq. (18):

$$C_6H_5Hg^+ + h^+_{VB}/HO^\bullet + H^+ \rightarrow\rightarrow C_6H_5OH + Hg^{2+} \quad (17)$$

$$C_6H_5OH + h^+_{VB}\ (HO^\bullet) \rightarrow \ldots \rightarrow CO_2 + H_2O \quad (18)$$

It was confirmed that Hg(II) behaves as a better oxidant than oxygen for mineralization. Hg(II) removal and mineralization were more favorable in the absence of oxygen and at pH 11, where HgO is formed together with Hg(0). Phenol was detected for both, PMA and PMC, as a product of the photocatalytic reaction; the very dangerous alkylmercury species were not formed. However, reaction under UV-light should be carried out until reaching complete mineralization to avoid the risk of formation of noxious intermediates after the treatment. Phenol concentration and mercury speciation in the filtrate was followed by a HPLC method developed by the group [38].

Later, Miranda et al. [37] studied the TiO_2 photocatalytic degradation of phenylmercury (λ = 300–400 nm), analyzing the effect of pH. Almost 100 % mercury reduction was obtained under N_2 at pH 10 and 0.35 g L^{-1} TiO_2 after 30 min UV irradiation, and after 40 min under saturated O_2. Phenol and diphenylmercury were identified as intermediate oxidation products. A major fraction of the reduced mercury was removed as metallic vapor by gas stripping, whereas a minor fraction was adsorbed on the catalyst surface, probably as $Hg(OH)_2$.

Yepsen et al. [39] reported recently the removal of thiomersal, a common antifungal and antibacterial agent used in vaccines. Thimerosal photocatalytic degradation will be studied in a next paper.

To our best knowledge, no report exists on $C_2H_5Hg^+$ degradation by heterogeneous photocatalysis. In this paper, this system is studied, focusing on the kinetic behavior system and its dependence on the initial concentration of the pollutant. A reaction mechanism has been proposed.

2. Experimental

2.1. Materials

TiO_2 was Evonik P25 Aeroxide (P25) and was used without further purification. According to the literature, P25 presents a surface area in the 48−56 m^2 g^{-1} range, primary particle size around 20−50 nm, and a phase composition of 70–80 % anatase and 30−20% rutile [40]. C_2H_5HgCl (Alfa Aesar, purity > 95 %) was used as pollutant source. All other reagents were at least of reagent grade and used without further purification. Solutions were prepared with Milli-Q water (resistivity =18 MΩ.cm). Diluted NaOH (≈ 0.1 M) was used to adjust pH before the photocatalytic runs.

2.2. Adsorption and photocatalytic experiments

Runs were carried out in a recirculating system (1.5 L min^{-1} flow rate) consisting of an annular reactor (415 mm-length, 35 mm-external diameter, 85 mL total volume), a peristaltic pump and a thermostatted (25 °C) cylindrical reservoir provided with magnetic stirring. A black-light tubular UV lamp (FLBLB, Toshiba Electric, 15 W, 300 < λ/nm < 400, maximum emission at 352 nm) was installed inside the annular reactor as the source of illumination. Actinometric measurements were performed by the ferrioxalate method. The incident photon flux per unit of volume ($q^\circ_{n,p}/V$) was 2.87 μeinstein s^{-1} L^{-1}. During adsorption and photocatalytic experiments in the presence of O_2, the reaction was conducted with the reactor open to air ($[O_2] \approx 8$ mg L^{-1} during adsorption in the dark, $[O_2] \approx 3$ mg L^{-1} under irradiation); in the experiments performed in the absence of O_2 ($[O_2] < 0.05$ mg L^{-1}), a water-saturated N_2 stream was bubbled in the suspension at 0.4 L min^{-1} throughout the experiment.

In all cases, 0.5 g of the catalyst was suspended in 500 mL of an aqueous solution of C_2H_5HgCl at the desired initial concentration, and adjusted at 4.2 with diluted NaOH. Then, the suspension was ultrasonicated for 2 min and recirculated in the dark for 30 min before irradiation to assure the substrate - surface equilibrium. The extent of adsorption of $C_2H_5Hg^+$ onto TiO_2 was determined by measuring $C_2H_5Hg^+$ concentrations in the solution before TiO_2 addition and in the filtrate (see below) after 30 min of recirculating in the dark. No pH changes were detected even after 60 min of stirring in the dark. During the $C_2H_5Hg^+$ photocatalytic degradation experiments, pH was left to vary freely from the initial value of 4.2; usually, a small decrease on pH was observed, probably related with the generation of carboxylic acids from the organic moiety ($3.7 \leq pH \leq 4.3$). Samples were periodically withdrawn and filtered through 25 mm diameter, 0.22 μm pore size, Millipore acetate cellulose filters. Duplicated runs were carried out for each condition, averaging the results; when differences between replicates was higher than 5%, triplicates were done and the two closer results averaged.

2.3. Analytical determinations

$C_2H_5Hg^+$ concentration and Hg speciation in the filtrate was followed by HPLC using a previously developed method [38]. Briefly, the mobile phase was composed of CH_3OH:CH_3CN:5 mM NaH_2PO_4 buffer (1:4:5) containing 0.1 mM 2-mercaptopropionic acid (2-MPA) to complex the different Hg species. A flow rate of 0.8 mL min^{-1} was employed, and UV detection at 220 nm was performed. The chromatographic system consisted of an Alltech 301 HPLC Pump, a 100-μL loop, a Thermo C18 column (5 μm, 15 cm × 4.6 mm) and a Spectra SYSTEM UV1000 detector. Data acquisition was processed with Konikrom software. Peak height was employed to quantify the concentration of the analytes. Detection limits were 108 μg L^{-1} for Hg^{2+}, 39 μg L^{-1} for CH_3Hg^+ and 42 μg L^{-1} for $C_2H_5Hg^+$.

The deposits on the recovered photocatalyst were analyzed by chemical reactions for identification of different products. A gray deposit, soluble in concentrated nitric acid, indicated metallic Hg [35,41]. The treatment of the deposit with 2.5 M KI, giving a filtrate absorbing at 323 nm, was assigned to the presence of HgO [42]. A pale gray deposit was an evidence of a mixture of metallic Hg and Hg_2Cl_2 [43]. Samples were also analyzed by X-ray diffraction (XRD) at room temperature, using a Philips PW- 3710 diffractometer and Cu-Kα radiation.

The mineralization degree was followed by total organic carbon analysis, using a Shimadzu 5000A TOC analyzer in the non-purgeable organic carbon mode (NPOC).

3. Results

3.1. Adsorption of ethylmercury over TiO_2

The amount of $C_2H_5Hg^+$ adsorbed over the TiO_2 photocatalyst (q_e) before the beginning of the photocatalytic experiment was calculated according to Eq. (19):

$$q_e = \frac{[C_2H_5Hg^+]_0 - [C_2H_5Hg^+]_e}{[TiO_2]} \quad (19)$$

where $[C_2H_5Hg^+]_0$ represents the $C_2H_5Hg^+$ concentration measured in solution before the addition of TiO_2 (see section 2.2), and $[C_2H_5Hg^+]_e$ is the $C_2H_5Hg^+$ concentration after 30 min of equilibrium in the dark with TiO_2 at pH 4.2. No further $C_2H_5Hg^+$ adsorption was observed at contact times longer than 30 min, as observed previously for $Hg(NO_3)_2$ [44] or $HgCl_2$ [45] treated with P25, although Ghasemi et al. [46] reported that a minimum of 7 h was required to achieve the Hg(II) adsorption equilibrium over TiO_2 at pH 8 starting from $HgCl_2$. Interestingly, Lenzi et al. [25] found that $HgCl_2$ adsorption over TiO_2 at pH 4 was almost negligible. The results of $C_2H_5Hg^+$ adsorption over TiO_2 can be observed in Fig. 1 and indicate a higher than linear increase in q_e with the $C_2H_5Hg^+$ concentration. For $[C_2H_5Hg^+] \leq 1$ mM, the values of q_e are lower than those found for $HgCl_2$ adsorption over P25 under similar conditions of pH and $[TiO_2]$ [45], being the difference more significant as $[C_2H_5Hg^+]$ decreases. As no previous studies were performed regarding $C_2H_5Hg^+$ or CH_3Hg^+ adsorption on TiO_2, four adsorption models (two parameters), commonly used to evaluate Hg(II) adsorption over TiO_2 and/or TiO_2 based materials [45–47], were used here to fit the experimental data: Langmuir (Eq. (A17)), Freundlich (Eq. (A18)), Temkin (Eq. (A19)) and Dubinin-Radushkevich (D-R) (Eqs. (A20) and (A21)) isotherms. Other isotherms could be also tested but they are less used (e.g., [48]). The values of the parameters, together with the correlation coefficients R^2, can be observed in Table 1.

As can be observed from Fig. 1 and Table 1, the Freundlich model gives the best fit for the obtained results, in agreement with that found by Ghasemi et al. [46] for $HgCl_2$; however, a value of $n < 1$ was obtained for $C_2H_5Hg^+$, indicating that the adsorption over P25 in aqueous suspension for this species is not favorable. The Langmuir isotherm also gave a good fitting ($R^2 = 0.98$), but the K_L value obtained (0.1 mM^{-1}) indicates that, for all the studied range, $K_L \times [C_2H_5Hg^+]_e$ is almost one order of magnitude or smaller than 1 ($9.64 \times 10^{-3} \leq K_L \times [C_2H_5Hg^+]_e \leq 0.137$). Then, according to Eq. (A17), an almost linear relation between $[C_2H_5Hg^+]_e$ and q_e is obtained (black dashed line in Fig. 1); besides, with this K_L value, a 90 % coverage of the TiO_2 surface ($q_e/q_{mL} = 0.9$) could only be obtained at $[C_2H_5Hg^+]_e \geq 90$ mM (calculated from Eq. (A17)), i.e., 24 times higher than the $C_2H_5Hg^+$ solubility limit (3.76 mM [49]), indicating that the q_{mL} value obtained may be not realistic. Regarding Temkin and D–R models, Fig. 1 and Table 1 clearly show that those models do not fit the experimental data.

Table 1
Fitting parameters and correlation coefficients of the results included in Fig. 1 to the Langmuir, Freundlich, Temkin and Dubinin-Radushkevich adsorption isotherms (Eqs. A17) to (A21)).

Adsorption isotherm	Isotherm parameters		R^2
Langmuir	q_{mL}	0.61 ± 0.03 mmol g^{-1}	0.98
	K_L	0.1 ± 0.005 mM^{-1}	
Freundlich	n	0.94 ± 0.08	0.99
	K_F	0.054 ± 0.002 $mM^{-0.06}$ L g^{-1}	
Temkin	b	100 ± 20 g J $mmol^{-2}$	0.84
	K_T	9 ± 2 mM^{-1}	
D–R	q_{mDR}	0.06 ± 0.01 mmol g^{-1}	0.88
	K_{DR}	$8.0.10^{-8} \pm 1.10^{-8}$ mol^2 J^{-2}	

3.2. Photocatalytic experiments of C_2H_5HgCl at different initial concentrations

Experiments with different initial C_2H_5HgCl concentrations ($0.1 \leq [C_2H_5Hg^+]_0 \leq 1.5$ mM) were performed with the reactor open to air and at initial pH of 4.2, the pH of the 0.1 mM $C_2H_5Hg^+$ solution in pure water. In all cases, the amount of the compound adsorbed in the dark (see Section 3.1) was discounted to analyze only the effect of light on the photocatalytic transformation. The results are shown in Fig. 2.

The UV–vis spectrum of a 1.5 mM solution of $C_2H_5Hg^+$ at pH 4.2 is shown in Section A3, Fig. A1. It can be seen that the compound only absorbs at wavelengths lower than 250 nm and that the absorption in the range of emission of the lamp ($300 < \lambda/nm < 400$) is very low.

As it can be seen, the time required to remove $C_2H_5Hg^+$ increases when $[C_2H_5Hg^+]_0$ increases, indicating that the photocatalytic process does not follow a pseudo-first order kinetics; also, for a given $[C_2H_5Hg^+]_0$, the removal rates decrease as the degradation of $C_2H_5Hg^+$ takes place, indicating that the system does not follow either a zero-order kinetics. Then, a saturation kinetics, that approximates to zero-

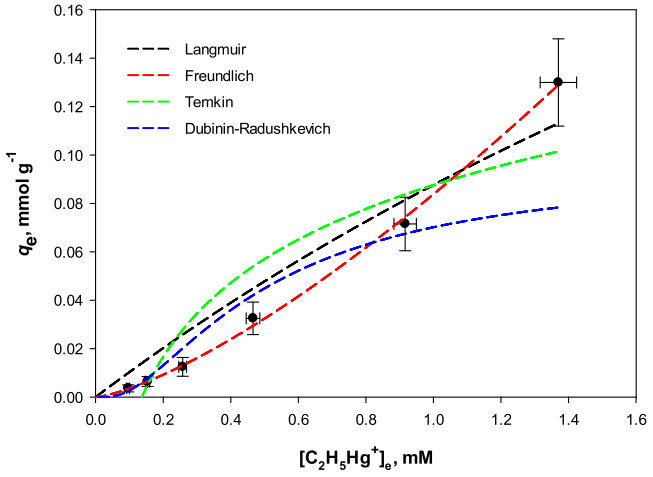

Fig. 1. Equilibrium adsorption of $C_2H_5Hg^+$ over P25. Conditions: $[C_2H_5Hg^+]_0 = 0.1$-1.5 mM, $[TiO_2] = 1$ g L^{-1}, $T = 25$ °C, pH_0 4.2, reactor open to air. Dashed lines represent the fitting of experimental data to Langmuir, Freundlich, Temkin and Dubinin-Radushkevich isotherms (Eqs. (A17) to (A21), respectively).

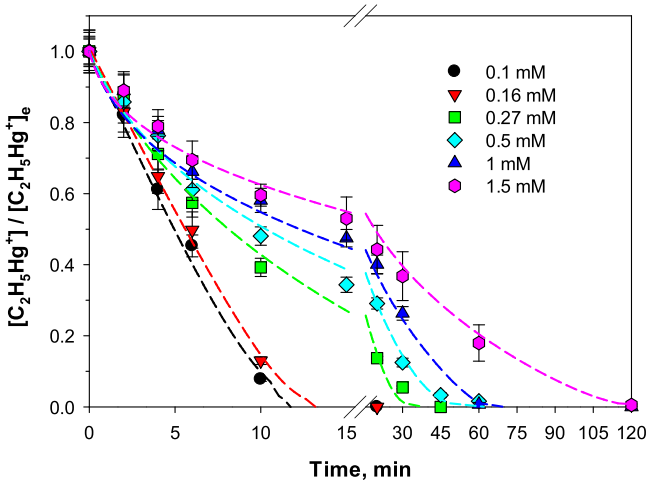

Fig. 2. Evolution of normalized mercury TiO_2-photocatalytic concentration starting from C_2H_5HgCl. Conditions: $[C_2H_5Hg^+]_0 = 0.1$-1.5 mM, $[TiO_2] = 1$ g L^{-1}, $T = 25$ °C. pH_0 4.2, reactor open to air, $q^0_{n,p}/V = 2.87$ μeinstein s^{-1} L^{-1}. Dashed lines represent the fitting of experimental data to Eq. (24). Error bars represent the standard deviation between duplicates.

order rates at high concentrations and pseudo-first order rates at low concentrations, usually used to describe degradation kinetics in photocatalytic experiments with TiO_2 [50], and represented by Eq. (20), was used to fit the kinetic results:

$$r = -\frac{d[C_2H_5Hg^+]}{dt} = \frac{k \times K_{C_2H_5Hg} \times [C_2H_5Hg^+]}{\sum_i K_{(i)} \times [i] + 1} \quad (20)$$

where k is the photocatalytic rate constant for $C_2H_5Hg^+$ degradation, $K_{(i)}$ is the affinity (or binding) constant for all compounds competing for the same TiO_2 surface sites under irradiation and $K_{C_2H_5Hg}$ is the affinity constant for $C_2H_5Hg^+$. Although this empirical behavior does not mean that the mechanism involves adsorption processes onto the catalyst surface [51,52], it is supposed that the pollutant have, at least, to be close to catalyst surface to allow the occurrence of the reaction. If it is assumed that the degradation intermediates have less affinity than $C_2H_5Hg^+$ for the TiO_2 surface, that their concentrations are low compared with that of $C_2H_5Hg^+$, and/or that they are adsorbed onto different TiO_2 sites, then $\sum_i K_{(i)} \times [i] \approx K_{C_2H_5Hg} \times [C_2H_5Hg^+]$, and Eq. (20) can be simplified to Eq. (21):

$$r = -\frac{d[C_2H_5Hg^+]}{dt} = \frac{k \times K_{C_2H_5Hg} \times [C_2H_5Hg^+]}{K_{C_2H_5Hg} \times [C_2H_5Hg^+] + 1} \quad (21)$$

According to Eq. (21), r can be approximated to a pseudo-first order model at low $[C_2H_5Hg^+]$, and to a pseudo-zero order model at high $[C_2H_5Hg^+]$; however, the results of Fig. 2 show the opposite behavior: at $[C_2H_5Hg^+] \leq 0.16$ mM, the evolution follows an almost zero-order behavior, which is deviated to a pseudo-first order model at higher $[C_2H_5Hg^+]$. This deviation from the model can be related with the deactivation of the photocatalyst, previously observed by Aguado et al. [23] during their experiments of Hg(II) nitrate photocatalytic reduction. Then, in order to consider the deactivation of the photocatalyst, in Eq. (21) the parameter k was replaced by a photocatalytic kinetic constant k_0 modified by a deactivation function σ_d, according to Eq. (22):

$$k = k_0 \times \sigma_d = \frac{k_0}{(1 + \alpha([C_2H_5Hg^+]_e - [C_2H_5Hg^+]))^2} \quad (22)$$

In Eq. (22), an hyperbolic deactivation function was chosen, the same used by Aguado et al. [23], where α is the deactivation constant (mass TiO_2/mass of $C_2H_5Hg^+$; as $[TiO_2]$ was always 1 g L^{-1}, the units used here were mM^{-1} of $C_2H_5Hg^+$), and $[C_2H_5Hg^+]_e$-$[C_2H_5Hg^+]$ represents the amount of $C_2H_5Hg^+$ degraded, which in turn is related to the amount of Hg(0) over the photocatalyst, the species responsible for the deactivation (see below). By replacing Eq. (22) in Eq. (21), Eq. (23) is obtained.

$$r = -\frac{d[C_2H_5Hg^+]}{dt} = \frac{k_0 \times K_{C_2H_5Hg} \times [C_2H_5Hg^+]}{(1 + \alpha([C_2H_5Hg^+]_e - [C_2H_5Hg^+]))^2 (K_{C_2H_5Hg} \times [C_2H_5Hg^+] + 1)} \quad (23)$$

Integrating Eq. (23), Eq. (24) is obtained:

$$t = \frac{\left(K_{C_2H_5Hg} \times (\alpha \times A + 1)^3\right)}{3 \times \alpha} - 0.5 \times (\alpha \times A + 1)^2 - B \times (\alpha \times A + 1) - B^2 \times \ln(\alpha \times [C_2H_5Hg^+]) - C \quad (24)$$

where $A = ([C_2H_5Hg^+]_e - [C_2H_5Hg^+])$, $B = (\alpha \times [C_2H_5Hg^+]_e + 1)$, and $C = \frac{K_{C_2H_5}}{3 \times \alpha} - 0.5 - B - B^2 \times \ln(\alpha \times [C_2H_5Hg^+]_e)$.

The value of $[C_2H_5Hg^+]_e$ was set constant and equal to the value of $[C_2H_5Hg^+]$ in solution after the adsorption equilibrium was reached for each $[C_2H_5Hg^+]_0$ used, as shown in Fig. 2; the value of $[C_2H_5Hg^+]_e$ and the fitting parameters (k_0, $K_{C_2H_5Hg}$ and α) of the experimental points of Fig. 2 with Eq. (24) are displayed in Table 2.

Table 2
$C_2H_5Hg^+$ concentration in solution after adsorption equilibrium was reached ($[C_2H_5Hg^+]_e$), and fitting parameters and correlation coefficients of Eq. (24) for the experimental results with different $[C_2H_5Hg^+]_0$ shown in Figs. 2 and 4. The value of the experiment with $[C_2H_5Hg^+]_0 = 0.5$ mM under N_2 bubbling was also included.

$[C_2H_5Hg^+]_0$ (mM)	$[C_2H_5Hg^+]_e$ (mM)	$k_0 \times 10^3$ (mM min^{-1})	$K_{C_2H_5Hg}$ (mM^{-1})	α (mM^{-1})	R^2
0.1	0.096 ± 0.004	11.1 ± 0.3	90 ± 20	0	0.990
0.16	0.154 ± 0.006	15.1 ± 0.3	90 ± 30	0	0.996
0.27	0.26 ± 0.01	29 ± 2	73 ± 30	4.5 ± 0.4	0.982
0.5	0.47 ± 0.02	54 ± 2	50 ± 15	4.5 ± 0.2	0.990
0.5 (N_2 bubbling)	0.47 ± 0.02	120 ± 10	50 ± 10	4.5 ± 0.2	0.982
1	0.92 ± 0.03	188 ± 4	90 ± 30	4.5 ± 0.1	0.995
1.5	1.37 ± 0.05	289 ± 7	60 ± 20	4.5 ± 0.1	0.993

As can be observed from Fig. 2 and R^2 values in Table 2, Eq. (24) gives a proper fitting of the temporal evolution of $C_2H_5Hg^+$; however, for $[C_2H_5Hg^+]_0 \leq 0.16$ mM, a value of $\alpha = 0$ is obtained, indicating that no deactivation is taking place at these low concentrations, and that the system follows a normal saturation kinetics (the integrated form of Eq. (21)).

The values of $K_{C_2H_5Hg}$ obtained are rather constant, as all are within the error reported in the fitting. An average value of 76 ± 17 mM^{-1} for the different $[C_2H_5Hg^+]_0$ can be obtained; thus, under most conditions, $K_{C_2H_5Hg} \times [C_2H_5Hg^+] >> 1$, and Eq. (23) is reduced to almost zero-order kinetics with hyperbolic deactivation. This can be clearly observed for the experiments at $[C_2H_5Hg^+]_0 \leq 0.16$ mM, where, as indicated above, no deactivation is observed, and the experimental points follow an almost straight line.

On the other hand, the values of k_0 increase steadily as $[C_2H_5Hg^+]_0$ increases; the dependence of this parameter with q_e and with $[C_2H_5Hg^+]_e$ is analyzed in Fig. 3. The results indicate that there is an almost linear relationship between k_0 and q_e, the experimental values fitting to a line within the experimental error (black dashed line in Fig. 3). A direct correlation between k_0 and $[C_2H_5Hg^+]_e$ can also be observed, but, in this case, the linear fitting is not so good. The better correlation of k_0 with q_e than with $[C_2H_5Hg^+]_e$ can be rationalized considering that $C_2H_5Hg^+$ degradation is initiated on the TiO_2 surface, and that a higher $C_2H_5Hg^+$ surface concentration increases the possibility that the generated e^-_{CB} and h^+_{VB} react with this pollutant, as it will pointed out in section 4.2. As the relationship between q_e and $[C_2H_5Hg^+]_e$ is not linear (see section 3.1), an increase in $[C_2H_5Hg^+]_e$ does not give a linear increase in q_e, and thus, the correlation of k_0 with $[C_2H_5Hg^+]_e$ is not straightforward, but it is mediated by the adsorption equilibrium.

No CH_3Hg^+ formation was detected under any of the initial $C_2H_5Hg^+$ concentrations studied. NPOC evolution in solution during the photocatalytic removal of C_2H_5HgCl ($[C_2H_5Hg^+]_0 = 0.5$ mM, pH 4.2, reactor open to air) is presented in Section A4, Fig. A2. Carbon decay is fast, and continues even after the complete degradation of $C_2H_5Hg^+$, indicating that the organic products formed during the photocatalytic reaction can be further degraded; after 180 min, an 80 % of mineralization was achieved.

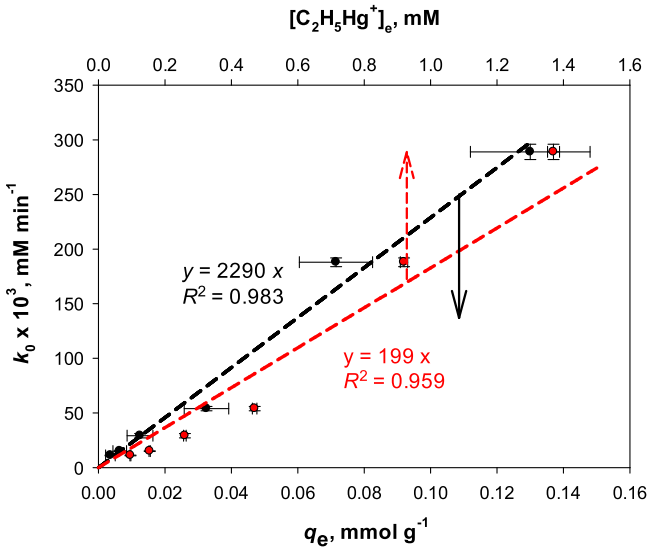

Fig. 3. Dependence of the photocatalytic kinetic constant k_0 (shown in Table 2) with q_e and $[C_2H_5Hg^+]_e$, both at initial times. Dashed lines show the linear regression of each series, passing through the origin. Conditions of Fig. 2.

3.3. Effect of pH and of the presence of oxygen

Comparative experiments of removal of 0.5 mM C_2H_5HgCl solution with the reactor open to air or under N_2 bubbling, now monitoring mercury speciation ($C_2H_5Hg^+$ and Hg^{2+}), show that the decay of C_2H_5Cl is faster in the absence of O_2 (Fig. 4). As indicated in section 3.2, no CH_3Hg^+ formation was detected neither in the presence nor in the absence of O_2.

As indicated in Table 2, in the absence of dissolved O_2, the temporal evolution of the $C_2H_5Hg^+$ concentration could also be fitted with Eq. (24), with $k_0 = 120 \times 10^{-3}$ mM s^{-1} ($R^2 = 0.982$), being $K_{C_2H_5Hg}$ and α identical to the values obtained with the reactor open to air at the same $[C_2H_5Hg^+]_0$. The value of k_0 shows a significant increase, reflecting the increase in the degradation rate in the absence of O_2, which can be clearly appreciated in Fig. 4.

Fig. 4 shows that at 60 min, with and without O_2, $C_2H_5Hg^+$ has been almost completely degraded (faster without O_2). Hg(II) remains in solution, mainly as $HgCl_2$ (99.6 % of total Hg(II) in solution) as it can be calculated from the equilibrium constants [24] and total $[Cl^-] \approx 0.5$ mM (see section A5). Hg^{2+} concentration was almost constant even after 180 min of irradiation (see inset in Fig. 4), with a value around 0.05 mM, under both conditions (0.053 +/- 0.003 mM under N_2, and 0.047 +/- 0.005 under O_2, Fig. 4). However, the temporal evolution is quite different as, under N_2, a fast increase in Hg(II) is observed at initial times (0.076 mM at 6 min) followed by a slow decrease, even after complete $C_2H_5Hg^+$ removal. When O_2 was present, the highest Hg(II) concentration (0.066 mM) was obtained after complete $C_2H_5Hg^+$ degradation (at 60 min). The slow photocatalytic removal of Hg(II) can be related to the photocatalyst deactivation mentioned before, and agrees with previous reports that indicate that the photocatalytic removal of Hg^{2+} is slow at acidic pH in the absence of donors [14,16,24].

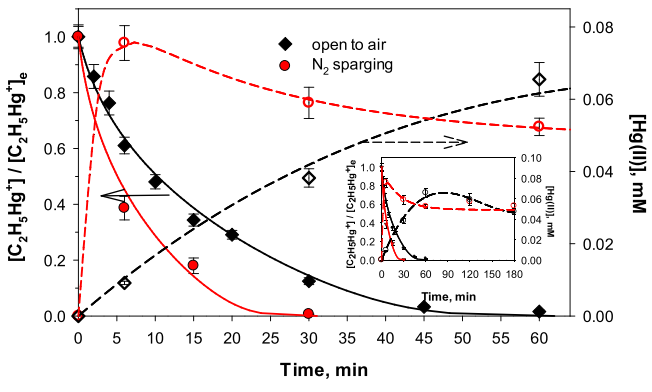

Fig. 4. Influence of dissolved O_2 on the photocatalytic C_2H_5HgCl treatment. Open symbols: free Hg^{2+} in solution. Conditions: $[C_2H_5HgCl]_0 = 0.5$ mM, $[TiO_2] = 1$ g L^{-1}, $T = 25$ °C, pH$_0$ 4.2, $q^\circ_{n,p}/V = 2.87$ μeinstein s^{-1} L^{-1}. Solid lines: fitting of $[C_2H_5Hg^+]$ to Eq. (24). Dashed lines are only for visualization and do not correspond to any fitting model. Inset: extension up to 180 min.

The photocatalytic conversion of C_2H_5HgCl under N_2 at pH 4.2 produced a deposit composed of a Hg(0) and Hg_2Cl_2 mixture. Calomel was detected by XRD (the wide and low intensity peak is at $2\theta = 21.45$ corresponding to the (101) diffraction), together with anatase (JCPDS No. 21-1272) and rutile (JCPDS No. 75-1753) peaks (Fig. 5) in agreement with previous papers of the group [14,36]. Hg(0) was visually identified as a dark grey solid, soluble in HNO_3(c) (see Section 2.3). The influence of O_2 on the obtained deposits on TiO_2 at the end of the treatment is proved, as only Hg(0) was observed under this condition.

As previous papers have demonstrated that Hg(II) removal from inorganic Hg and organomercurials is higher at basic pH [14,36], a separate experiment was done with 0.5 mM $C_2H_5Hg^+$ under similar conditions, open to air, but increasing pH to 10 at 120 min. Under this situation, no $C_2H_5Hg^+$ remained in solution, with an acceleration of Hg (II) removal. Total removal of mercury species ($[C_2H_5Hg^+] < 1.8 \times 10^{-4}$ mM, $[Hg^{2+}] < 5.4 \times 10^{-4}$ mM) was obtained at 240 min of reaction. Only initial and final values are reported.

4. Discussion

4.1. Adsorption of $C_2H_5Hg^+$ over P25

It has been reported that, in the case of mercury chloride, which gave generally much higher photocatalytic mercury removal than other mercury compounds, the dominant species is always uncharged: $HgCl_2$ at pH < 6 and $Hg(OH)_2$ at pH > 6 [21]; consistently, a rather constant adsorption in the dark was found between pH 3 and 11 for $HgCl_2$ [14, 53].

As indicated in Section 3.1, adsorption of $C_2H_5Hg^+$ over P25 is best fitted by the Freundlich isotherm with $n < 1$, indicating that the adsorption is not favorable, and/or that competitive adsorption by water molecules is taking place; this is also reflected by the rather low value of K_L obtained using the Langmuir isotherm (0.1 mM^{-1}), much smaller than the values obtained for other substances that are readily adsorbed

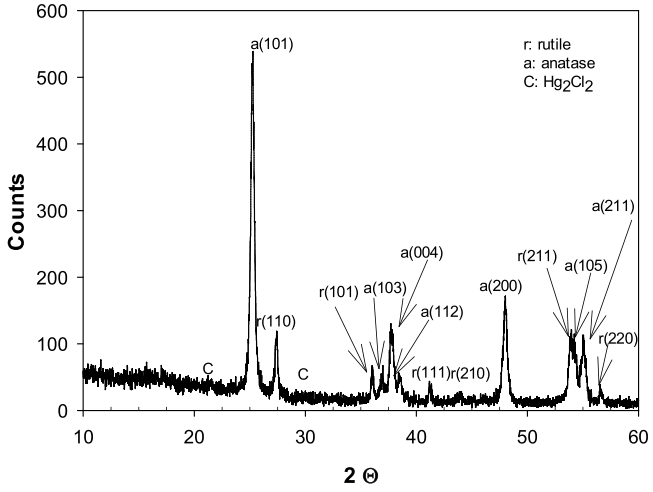

Fig. 5. XRD pattern of the recovered TiO_2 after photocatalysis of C_2H_5HgCl under N_2. Conditions of Fig. 4.

over P25 at acid pH, such as Cr(VI) (12 mM^{-1} [54]) and carboxylic acids (40 to 8000 mM^{-1} [55]). The unfavorable adsorption can be ascribed to electrostatic repulsion as, at the working pH (4.2), $C_2H_5Hg^+$ is largely found as the cationic species ($pK_a = 4.90$) [56], and the P25 surface is positively charged (pH of PZC for P25 $TiO_2 = 6–7$ [45]); the authors of reference [24] arrived to the same conclusions regarding Hg(II) adsorption over TiO_2. Another possible explanation is that, as q_e increases, the organic moiety of $C_2H_5Hg^+$ makes the surface less hydrophilic, favoring $C_2H_5Hg^+$ adsorption, a phenomenon called "cooperative adsorption" [57], where the adsorbate enhances the adsorption of more adsorbate molecules, and this is consistent with $n < 1$ in the Freundlich isotherm [48] (see Section A2, Appendix A). This behavior has been observed for Hg(II) adsorption over γ-Fe_2O_3 nanoparticles [58], and for thiomersal adsorption onto activated carbon, especially at pH conditions where both thiomersal and the carbon adsorbent are negatively charged [59]. The results of Fig. 1 correspond to the $C_2H_5Hg^+$ adsorption before the inflection point of an S-shaped [57] (Giles classification [60]) or Type V [61] (IUPAC classification [62]) isotherms, or with a Type III isotherms [61]. Finally, it can be considered that the highest $[C_2H_5Hg^+]_e$ values are close to the solubility limit, which, as said, is lower than 3.76 mM [49]; this favors $C_2H_5Hg^+$ multilayer adsorption, and is consistent with a cooperative adsorption [61]. The adsorption energy E, calculated from the Dubinin-Radushkevich isotherm using Eqs. (A20) and (A21), was 2.50 kJ mol^{-1}, clearly indicating physical adsorption [46].

4.2. Photocatalytic results

In the present work, no control experiments were performed to evaluate the possible contribution of direct $C_2H_5Hg^+$ photolysis to the $C_2H_5Hg^+$ degradation, and no reference was found in the literature regarding $C_2H_5Hg^+$ stability under UV irradiation at $\lambda > 300$ nm. However, considering that: 1) Zhang et al. [28] indicate that CH_3Hg^+, a compound with a UV–vis spectrum similar to that of $C_2H_5Hg^+$, was stable under simulated sunlight in pure water; 2) under the irradiation wavelengths used in this work (300−400 nm), the absorbance of $C_2H_5Hg^+$ is almost negligible (see Fig. A1); and 3) P25 absorbance is high (especially at $\lambda < 375$ nm [63]), it can be concluded that the contribution of the $C_2H_5Hg^+$ photolysis can be neglected.

As can be observed from the results of Fig. 2 and Table 2, during a given run, the temporal evolution of $C_2H_5Hg^+$ can be fitted to a saturation, Langmuir-Hinshelwood (LH) type kinetics (Eq. (20)), as observed for TiO_2 photocatalytic degradation of other organomercurial compounds [34,36,37]); this indicates that $C_2H_5Hg^+$ adsorption is a critical step in the photocatalytic degradation mechanism [37]. An average value of 76 ± 17 mM^{-1} was obtained for the affinity constant $K_{C_2H_5Hg}$, similar to the value obtained for CH_3Hg^+ (288 mM^{-1} [34]), but very different from the values reported for phenylmercury: 1.56 mM^{-1} by de la Fournière et al. [36] (calculated as k_1/k_0 mM^{-1} from the values there reported: $k_1 = 3.9 \times 10^{-4}$ s^{-1}, and $k_0 = 2.5 \times 10^{-7}$ M s^{-1}); and 7.1×10^5 mM^{-1} by Miranda et al. [34]. The value of $K_{C_2H_5Hg}$ was much higher than that obtained for K_L in the dark (0.1 mM^{-1}, Table 1), and this difference can be ascribed to changes that take place on the TiO_2 surface under irradiation and/or to the fact that $K_{C_2H_5Hg}$ is a phenomenological constant [51], which only indicates the influence of $C_2H_5Hg^+$ concentration in solution on the photocatalytic degradation rate (as $K_{C_2H_5Hg}$. increases, r is less dependent on $[C_2H_5Hg^+]$). No changes on $K_{C_2H_5Hg}$ where obtained when working under N_2 compared with the experiment in the presence of O_2 at $[C_2H_5Hg^+]_0 = 0.5$ mM, reflecting that the effect of $C_2H_5Hg^+$ concentration in solution on the kinetic behavior was identical under both conditions, despite the differences in $C_2H_5Hg^+$ photocatalytic degradation rate.

At $[C_2H_5Hg^+]_0 \geq 0.27$ mM, a deviation from this model is observed, with a decrease of the $C_2H_5Hg^+$ photocatalytic degradation rate more pronounced than the expected from the LH model. As said, this can be ascribed to partial TiO_2 deactivation caused by Hg(0) deposition, as previously reported for Hg(II) photocatalytic reduction [23]. By including the hyperbolic deactivation function σ_d to the photocatalytic rate constant (k) (Eq. (22)), a very good fitting was obtained for all experiments performed at $[C_2H_5Hg^+]_0 \geq 0.27$ mM with Eq. (24), being the photocatalytic kinetic constant k_0 the only parameter that changed significantly and showing an almost linear correlation with q_e; this finding reinforces the assumption that $C_2H_5Hg^+$ photocatalytic degradation is initiated, at least to a large extent, on $C_2H_5Hg^+$ adsorbed onto the TiO_2 surface. Although the LH model has been used before to fit the photocatalytic destruction of organomercurial compounds [34,36,37], only initial degradation rates were evaluated in those works. Under similar experimental conditions, the values of k_0 of Table 2 were at least one order of magnitude higher than those reported for CH_3Hg^+ [34], most probably due to the higher efficiency of the photocatalytic reactor used here. For phenylmercury, the lower k_0 values obtained are similar to those reported by de la Fournière et al. [36] (15×10^{-3} mM min^{-1}) and Miranda et al. [37] (19.8×10^{-3} mM min^{-1}). The value of k_0 under N_2 was twice the value obtained when O_2 was present, confirming that $C_2H_5Hg^+$ photocatalytic degradation is more efficient in the absence of O_2; the reasons for this effect will be analyzed below.

As mentioned before, at any $[C_2H_5Hg^+]_0$ value $\geq$ 0.27 mM, a continuous decrease in $C_2H_5Hg^+$ degradation rate is appreciated despite the system should have a pseudo zero-order behavior according to the high $K_{C_2H_5Hg}$ values obtained ($\approx$ 76 mM^{-1}); this decrease can be associated with the competition between $C_2H_5Hg^+$ and its degradation by-products for surface active sites, and/or to the deposition of insoluble Hg species like Hg(0) and Hg_2Cl_2, which would block $C_2H_5Hg^+$ and UV radiation, agglomerate the TiO_2 nanoparticles decreasing the reaction surface and serve as h^+_{VB}-e^-_{CB} recombination centers [14,23,29,34]. The value of α (4.5 mM^{-1}, Table 2) is equivalent to 20 g TiO_2/g $C_2H_5Hg^+$ degraded, as can be calculated from the ratio between 4.5 mM^{-1} and the MW of $C_2H_5Hg^+$ (0.2296 g $mmol^{-1}$), multiplied by the TiO_2 concentration (1 g L^{-1}); if deposited Hg(0) is used for calculating α (considering that all degraded $C_2H_5Hg^+$ is transformed into Hg(0), neglecting Hg(II) in solution), by replacing the MW of $C_2H_5Hg^+$ by the atomic weight of Hg (0.20059 g $mmol^{-1}$), a value of 22 g TiO_2/g Hg(0) deposited can be obtained. This value of α is one order of magnitude higher that the values reported by Aguado et al. [23], indicating that the deactivation caused by Hg(0) is more significant for $C_2H_5Hg^+$ degradation than for Hg(II) reduction, and/or that other by-products formed (as Hg_2Cl_2 and organic compounds generated from the ethyl moiety degradation) are contributing to the photocatalyst deactivation. The fact that α had the same value in the presence and in the absence of O_2 supports the fact that the TiO_2 deactivation is directly proportional to the amount of $C_2H_5Hg^+$ degraded and transformed into Hg(0) (the main final product, either with or without O_2), and not by other factors, e.g., reaction time, impurities present in the system, etc. Also, it indicates that the tiny amounts of Hg_2Cl_2 formed under N_2 have only a minor contribution to TiO_2 deactivation, if any at all.

It has been reported that, initially, the Hg(II) photocatalytic reduction rate is increased once small amounts of Hg(0) are deposited over the TiO_2, either by e^-_{CB} trapping by Hg(0), reducing thus h^+_{VB}-e^-_{CB} recombination [14], and/or by reaction (25) while further Hg deposition deactivates the photocatalyst [14,23]:

$$Hg(II) + Hg(0)_s \rightarrow Hg_2^{2+} \quad (25)$$

No initial increase in the $C_2H_5Hg^+$ degradation rate could be observed in the results shown in Fig. 3, and this can be explained considering that the decrease in the h^+_{VB}-e^-_{CB} recombination rate due to the Hg(0) deposition is not significant or, most probably, because the reaction represented by Eq. (25) does not involve $C_2H_5Hg^+$ and, thus, would not exert any effect on $C_2H_5Hg^+$ degradation.

In the present paper, it can be proposed that $C_2H_5Hg^+$ photocatalysis leads to Hg removal (Eqs. (26)–(33)), through both oxidative and

reductive mechanisms; the Hg(II) species involved were proposed according the equilibrium reactions included in section A5 (SD). The following reasons can explain the proposed mechanism:

1) $C_2H_5Hg^+$ removal takes place at a rather high rate under acidic conditions even in the presence of O_2 and in the absence of donors, while, under similar conditions, Hg(II) reduction is almost negligible [14,24].
2) Under N_2, the $C_2H_5Hg^+$ degradation rate increases; if only an oxidative mechanism would take place, the degradation rate should slow down or even completely stop, due to the absence of an electron acceptor.
3) According to Serpone et al. [29], the degradation rate of CH_3Hg^+ (a compound very similar to $C_2H_5Hg^+$) increased in the presence of methanol, indicating that the presence of a donor, capable of inhibiting the oxidative pathway, does not arrest the degradation rate.

Therefore, the main reaction mechanism can be proposed as:

$$C_2H_5Hg^+Cl^- + h^+_{VB}/HO^\bullet \rightarrow C_2H_5^\bullet + HgCl^+ (+ OH^-) \quad (26)$$

$$C_2H_5Hg^+Cl^- + h^+_{VB}/HO^\bullet \rightarrow C_2H_4Hg^{+\bullet}Cl^- + H^+ (+ H_2O) \rightarrow C_2H_4 + HgCl \quad (27)$$

$$2\ HgCl \rightarrow Hg_2Cl_2 \quad (28)$$

$$HgCl + O_2 \rightarrow HgCl^+ + O_2^{\bullet -} \quad (29)$$

$$HgCl \rightarrow HgCl^+ + e^-_{CB} \quad (30)$$

$$C_2H_5Hg^+ + e^-_{CB} \rightarrow C_2H_5Hg^\bullet \quad (31)$$

$$2\ C_2H_5Hg^\bullet \rightarrow (C_2H_5)_2Hg + Hg(0) \quad (32)$$

$$C_2H_5Hg^\bullet + H^+ + e^-_{CB} \rightarrow C_2H_6 + Hg(0) \quad (33)$$

Reactions (1)-(4) are also included in this mechanism.

In the degradation of phenylmercury, de la Fournière et al. [36] and Miranda et al. [37] proposed that the direct reaction of $HO^\bullet$ with $C_6H_5Hg^+$ gives phenol plus Hg^{2+}, a different case compared with $C_2H_5Hg^+Cl^-$, that neither has an aromatic ring nor a C=C double bond. Regarding the formation of Hg(I) by Eqs. (1) and (27), it should be remembered that, as already mentioned in Section 1, the formation of HgCl is feasible, as E^0 ($HgCl_2$/HgCl) is −0.47 V ([21] and references therein).

$C_2H_5^\bullet$ radicals formed in reaction (26) may react with O_2 to give the peroxide radical $C_2H_5O_2^\bullet$, which would end in CO_2 after the photocatalytic degradation (Eq. (34)), or would decay by disproportionation (Eq. (35)) or recombination (Eq. (36)) [64]; although very unlikely, the contribution of $C_2H_5^\bullet$ to $C_2H_5Hg^+$ (Eq. (37)) and/or Hg(II) (Eq. (38)) reduction by an electron-transfer mechanism cannot be completely ruled out, considering that it has been reported that this radical can reduce $[Co^{III}W_{12}O_{40}]^{5-}$ to $[Co^{II}W_{12}O_{40}]^{6-}$ ($E^\circ = 1.01$ V) [65]:

$$C_2H_5^\bullet + O_2 \rightarrow C_2H_5O_2^\bullet \rightarrow \rightarrow CO_2 + H_2O \quad (34)$$

$$2\ C_2H_5^\bullet \rightarrow C_2H_4 + C_2H_6 \quad (35)$$

$$2\ C_2H_5^\bullet \rightarrow C_4H_{10} \quad (36)$$

$$C_2H_5^\bullet + C_2H_5Hg^+ (+ H_2O) \rightarrow C_2H_5Hg^\bullet + C_2H_4\ (C_2H_5OH) + H^+ \quad (37)$$

$$C_2H_5^\bullet + HgCl_2 (+ H_2O) \rightarrow HgCl + C_2H_4\ (C_2H_5OH) + H^+ + Cl^- \quad (38)$$

When O_2 is present, a decrease on $C_2H_5Hg^+$ removal rate can be appreciated compared with the system under N_2 (Fig. 4), which can be related to the competition between $C_2H_5Hg^+$ and O_2 for e^-_{CB} (Eq. (9)) and to the reoxidation of $C_2H_5Hg^\bullet$ (Eq. (39)), with superoxide production in both cases; $O_2^{\bullet -}$ in turn will be further transformed to H_2O (Eq. (40)):

$$C_2H_5Hg^\bullet + O_2 \rightarrow C_2H_5Hg^+ + O_2^{\bullet -} \quad (39)$$

$$O_2^{\bullet -} + 2\ H^+ + e^-_{CB} \rightarrow H_2O_2 + e^-_{CB} \rightarrow HO^- + HO^\bullet \rightarrow H_2O \quad (40)$$

If the reactions proposed by Eqs. (26) and (27) were the main scavenging mechanism of $h^+_{VB}/HO^\bullet$, intense Hg_2Cl_2 signals should have been observed by XRD; the tiny amount of Hg_2Cl_2 detected under N_2 and the lack of signals when O_2 was present can be ascribed to Hg_2Cl_2 consumption by $C_2H_5Hg^\bullet$ (Eq. (41)), as proposed by Hush and Oldham ([66], see Eqs. (27) and (28) of that paper).

$$C_2H_5Hg^\bullet + ½\ Hg_2Cl_2 \rightarrow C_2H_5Hg^+ + Hg(0) + Cl^- \quad (41)$$

Then, the small amount of Hg_2Cl_2 detected under N_2 can be related with the Hg(II) photocatalytic reduction (decreasing from 0.076 mM at 5 min to 0.05 mM after 60 min, Fig. 4). This takes place after $C_2H_5Hg^+$ has been almost completely degraded, and thus, $C_2H_5Hg^\bullet$ is no longer formed. Botta et al. [14] reported that $HgCl_2$ is only partially reduced by the photocatalytic treatment under acid conditions and under N_2, being Hg_2Cl_2 (and Hg(0)) formed by successive monoelectronic reductions. When O_2 is present, the amount of Hg(II) reduced is smaller than under N_2 (from 0.066 mM at 60 min to 0.05 mM after 180 min), and this may be the reason for the lack of detection of Hg_2Cl_2 under this condition; despite Hg(II) reduction under acid conditions was reported to be negligible when O_2 is present [14,24], the organic fraction of $C_2H_5Hg^+$ could act as an organic donor, enabling the small Hg(II) reduction detected, as observed i.e. when formic acid was added [24]. Using stopped-flow, it has been determined that the second order reaction rate between trapped e^-_{CB} (e^-_{trap}) and Hg(II) ($1.89 \times 10^5\ M^{-1}\ s^{-1}$, [67]) is one order of magnitude higher than that between e^-_{trap} and O_2 ($2.1 \times 10^4\ M^{-1}\ s^{-1}$ [68]), indicating that the inhibition effect of O_2 is most probably related to the fast reoxidation of the Hg(0) clusters formed after Hg(II) reduction [67]. Indeed, Fig. 4 shows that Hg(II) concentration under O_2 still increases even when $C_2H_5Hg^+$ has been completely degraded, indicating that Hg(0) oxidation by O_2 and/or $h^+_{VB}/HO^\bullet$ is taking place.

The final concentration of Hg^{2+} obtained (0.05 mM) is much higher than the maximum allowed level set by the WHO [69] for water consumption (6 μg L^{-1} for inorganic Hg) and those established by the US-EPA and the Argentine legislation (2 and 1 μg L^{-1}, respectively) [2,70]). However, complete Hg(II) removal using TiO_2 under UV irradiation could be achieved by increasing the reaction pH up to 7–10 [14,25], where the insoluble and non-volatile HgO is formed by oxidation of metallic Hg, in the presence of oxygen [71] (Eq. (42)):

$$Hg(0) + ½\ O_2 \rightarrow HgO \quad (42)$$

Also, particular care should be taken regarding the possible stripping of Hg(0) when gas is sparged in the system, but this inconvenience can be overcome by using a Cu(0) powder filter that can retain 90 % Hg(0) as amalgam [34].

As mentioned above, no CH_3Hg^+ has been found as a product of Hg^{2+} methylation, which could be possible if compounds such as acetic acid, acetaldehyde, ethanol and methanol, compounds that, as mentioned before, could be formed during the photocatalytic degradation of the organic moiety of $C_2H_5Hg^+$, can generate methyl radicals under the range of UV irradiation (300–400 nm) used in our runs [8 and references therein], or after their own photocatalytic degradation. Fortunately, CH_3Hg^+, the most toxic mercury species [5,72] (responsible for the occurrence of the neurotoxic Minamata disease (1953–1960) among residents of the Minamata Bay in Japan, with 121 persons poisoned, 46 fatally from eating the contaminated fish [5]), was not detected among the products of $C_2H_5Hg^+$ photocatalytic degradation, indicating that, if formed by $h^+_{VB}/OH^\bullet$ attack on the organic moiety of $C_2H_5Hg^+$, it would be rapidly destroyed by the photocatalytic process.

5. Conclusions

As in similar works, TiO_2-photocatalytic degradation has been found once again convenient for the treatment of organomercurials. The

adsorption of $C_2H_5Hg^+$ over TiO_2 in the dark can be described as a physical process regarding the energy involved, and it could be properly fitted with the Freundlich isotherm with $n < 1$, reflecting a not favorable adsorption, with a cooperative adsorption taking place. The photocatalytic kinetics of $C_2H_5Hg^+$ degradation for the different conditions studied can be fitted to a saturation two parameter LH like model type kinetics, modified to include a parameter that accounted for the deactivation occurring by the poisoning of TiO_2 by the deposited Hg(0). This model could fit the experimental results in the $[C_2H_5Hg^+]_0$ studied range (0.1–1.5 mM) with only three parameters: 1) the photocatalytic kinetic constant k_0, directly related with the surface concentration of q_e, the amount of $C_2H_5Hg^+$ adsorbed over the TiO_2 and thus, dependent on $[C_2H_5Hg^+]_0$; 2) the affinity constant $K_{C_2H_5Hg}$; and 3) the deactivation constant α, only significant at $[C_2H_5Hg^+]_0 > 0.16$ mM, when a considerable amount of Hg(0) was deposited over the TiO_2. At $[C_2H_5Hg^+]_0 \geq 0.27$ mM, both $K_{C_2H_5Hg}$ and α were almost independent of $[C_2H_5Hg^+]_0$.

Under N_2 atmosphere, the photocatalytic degradation rate is more than twice that observed in the presence of O_2, indicating a strong O_2 inhibition, ascribed to a reoxidation of the $C_2H_5Hg^\bullet$ formed by reduction of $C_2H_5Hg^+$ by e^-_{CB}. By comparison with the treatment of phenylmercury salts reported in our previous article [36], the system described here has common pathways: reduction of Hg^{2+} through successive one-electron transfer reactions passing through mercurous forms and mineralization of the organic moiety. Mercury release from the organic structure is due to the attack of $HO^\bullet$ or h^+_{VB}, but also by a reduction mechanism, initiated by e^-_{CB} and partially inhibited by O_2.

Total destruction of $C_2H_5Hg^+$ is found before 120 min of treatment when following the temporal evolution of the mercury species, but mercury remains partially in solution as Hg^{2+}. This drawback can be solved by increasing pH after $C_2H_5Hg^+$ has been eliminated. In this way, international level quality standards for mercury species in water can be reached.

CRediT authorship contribution statement

Emmanuel M. de la Fournière: Methodology, Formal analysis. **Jorge M. Meichtry:** Conceptualization, Data curation, Formal analysis, Funding acquisition, Investigation, Methodology, Project administration, Supervision, Validation, Visualization, Writing - original draft, Writing - review & editing. **Eduardo A. Gautier:** Conceptualization, Data curation, Formal analysis, Funding acquisition, Investigation, Methodology, Project administration, Supervision, Validation, Visualization, Writing - original draft, Writing - review & editing. **Ana G. Leyva:** Conceptualization, Data curation, Formal analysis, Funding acquisition, Investigation, Methodology, Project administration, Supervision, Validation, Visualization, Writing - original draft, Writing - review & editing. **Marta I. Litter:** Conceptualization, Data curation, Formal analysis, Funding acquisition, Investigation, Methodology, Project administration, Supervision, Validation, Visualization, Writing - original draft, Writing - review & editing.

Declaration of Competing Interest

The authors declare that they have no known competing financial interests or personal relationships that could have appeared to influence the work reported in this paper.

Acknowledgements

This work was supported by Agencia Nacional de Promoción Científica y Tecnológica (ANPCyT) from Argentina under PICT-2011-0463 and PICT-2015-0208.

Appendix A. Supplementary data

Supplementary material related to this article can be found, in the online version, at doi:https://doi.org/10.1016/j.jphotochem.2021.113205.

References

[1] L. Ling, M. Fan, B. Wang, T. Zhang, Application of computational chemistry in understanding the mechanisms of mercury removal technologies: a review, Energy Environ. Sci. 8 (2015) 3109–3133, https://doi.org/10.1039/C5EE02255J.
[2] E.M. Nolan, S.J. Lippard, Tools and tactics for the optical detection of mercuric ion, Chem. Rev. 108 (2008) 3443–3480, https://doi.org/10.1021/cr068000q.
[3] G. Kaiser, G. Tolg, Mercury, in: O. Hutzinger (Ed.), The Handbook of Environmental Part A: Anthropogenic Compounds, Springer-Verlag, Vol. 3, Springer-Verlag, Berlin, 1980, pp. 1–58. Part A.
[4] F.M. D'Itri, The Environmental Mercury Problem, Chem. Rubber Co., Cleveland, OH, 1972.
[5] N. Serpone, E. Borgarello, E. Pelizzetti, Photoreduction and photodegradation of inorganic pollutants: II. Selective reduction and recovery of Au, Pt, Pd, Rh, Hg, and Pb, in: M. Schiavello (Ed.), Photocatalysis and Environment, Kluwer Academic Publishers, Dordrecht, 1988, pp. 527–565.
[6] L. Bensefa-Colas, P. Andujar, A. Descatha, Intoxication par le mercure, Rev. Med. Interne 32 (2011) 416–424, https://doi.org/10.1016/j.revmed.2009.08.024.
[7] Q. Wang, D. Kim, D.D. Dionysiou, G.A. Sorial, D. Timberlake, Sources and remediation for mercury contamination in aquatic systems, Environ. Pollut. 131 (2004) 323–336, https://doi.org/10.1016/j.envpol.2004.01.010.
[8] Y. Yin, B. Chen, Y. Mao, T. Wang, J. Liu, Y. Cai, G. Jiang, Possible alkylation of inorganic Hg(II) by photochemical processes in the environment, Chemosphere 88 (2012) 8–16, https://doi.org/10.1016/j.chemosphere.2012.01.006.
[9] T. Tomiyasu, H. Kodamatani, R. Imura, A. Matsuyama, J. Miyamoto, H. Akagi, D. Kocman, J. Kotnik, V. Fajon, M. Horvat, The dynamics of mercury near Idrija mercury mine, Slovenia: horizontal and vertical distributions of total, methyl, and ethylmercury concentrations in soils, Chemosphere 184 (2017) 244–252, https://doi.org/10.1016/j.chemosphere.2017.05.123.
[10] H. Kodamatani, S. Katsuma, A. Shigetomi, T. Hokazono, R. Imura, R. Kanzaki, T. Tomiyasu, Behavior of mercury from the fumarolic activity of Mt. Myoko, Japan: production of methylmercury and ethylmercury in forest soil, Environ. Earth Sci. 77 (2018) 478, https://doi.org/10.1007/s12665-018-7616-y.
[11] J.-D. Yeh, S. Chen, Heavy metallic and organometallic ions scavenging using silica-based adsorbent functionalized with ligands containing sulfur and nitrogen elements, J. Chin. Chem. Soc. 59 (2012) 98–106, https://doi.org/10.1002/jccs.201100322.
[12] R.D. Wilken, F. Nitschke, R. Falter, Possible interferences of mercury sulfur compounds with ethylated and methylated mercury species using HPLC-ICPMS, Anal. Bioanal. Chem. 377 (2003) 149–153, https://doi.org/10.1007/s00216-003-2090-z.
[13] H. Kodamatani, T. Tomiyasu, Selective determination method for measurement of methylmercury and ethylmercury in soil/sediment samples using high-performance liquid chromatography chemiluminescence detection coupled with simple extraction technique, J. Chromatogr. A 1288 (2013) 155–159, https://doi.org/10.1016/j.chroma.2013.02.004.
[14] S.G. Botta, D.J. Rodríguez, A.G. Leyva, M.I. Litter, Features of the transformation of Hg^{II} by heterogeneous photocatalysis over TiO_2, Catal. Today 76 (2002) 247–258, https://doi.org/10.1016/S0920-5861(02)00223-7.
[15] M.I. Litter, Heterogeneous photocatalysis: transition metal ions in photocatalytic systems, Appl. Catal. B: Environ. 23 (1999) 89–114, https://doi.org/10.1016/S0926-3373(99)00069-7.
[16] X. Domènech, W. Jardim, M. Litter, M, Tecnologías avanzadas de oxidación para la eliminación de contaminantes, in: M.A. Blesa, B. Sánchez Cabrero (Eds.), Eliminación De Contaminantes Por Fotocatálisis Heterogénea, Ediciones CIEMAT, Madrid, 2004, pp. 7–34.
[17] M. Litter, X. Domènech, H. Mansilla, Remoción de contaminantes metálicos, in: M. A. Blesa, B. Sánchez Cabrero (Eds.), Eliminación De Contaminantes Por Fotocatálisis Heterogénea, Ediciones CIEMAT, Madrid, 2004, pp. 163–187.
[18] M.I. Litter, Treatment of chromium, mercury, lead, uranium and arsenic in water by heterogeneous photocatalysis, Adv. Chem. Eng. 36 (2009) 37–67, https://doi.org/10.1016/S0065-2377(09)00402-5.
[19] M.I. Litter, Last advances on TiO_2-photocatalytic removal of chromium, uranium and arsenic, Current Opinion in Green Sustain. Chem. 6 (2017) 150–158, https://doi.org/10.1016/j.cogsc.2017.04.002.
[20] M.I. Litter, N. Quici, J.M. Meichtry, A.M. Senn, Photocatalytic removal of metallic and other inorganic pollutants, in: D.D. Dionysiou, G. Li Puma, J. Ye, J. Schneider, D. Bahnemann (Eds.), Photocatalysis: Applications, RSC Publishing, Royal Society, London, 2016, pp. 35–71.
[21] M.I. Litter, N. Quici, J.M. Meichtry, V.N. Montesinos, Photocatalytic treatment of inorganic materials with TiO_2 nanoparticles, in: H.S. Nalwa (Ed.), Encyclopedia of Nanoscience and Nanotechnology, Vol. 29, American Scientific Publishers, Valencia, California, 2018, pp. 303–336.
[22] P.V. Kamat, Manipulation of charge transfer across semiconductor interface. A criterion that cannot be ignored in photocatalyst design, J. Phys. Chem. Lett. 3 (2012) 663–672, https://doi.org/10.1021/jz201629p.
[23] M.A. Aguado, S. Cervera-March, J. Giménez, Continuous photocatalytic treatment of mercury(II) on titania powders, Kinetics and catalyst activity, Chem. Eng. Sci. 50 (1995) 1561–1569, https://doi.org/10.1016/0009-2509(95)00001-L.
[24] X. Wang, S.O. Pehkonen, A.K. Ray, Photocatalytic reduction of Hg(II) on two commercial TiO_2 catalysts, Electrochim. Acta 49 (2004) 1435–1444, https://doi.org/10.1016/S0013-4686(03)00907-1.

[25] M.J. López-Muñoz, J. Aguado, A. Arencibia, R. Pascual, Mercury removal from aqueous solutions of $HgCl_2$ by heterogeneous photocatalysis with TiO_2, Appl. Catal. B: Environ. 104 (2011) 220–228, https://doi.org/10.1016/j.apcatb.2011.03.029.

[26] G. Lenzi, C. Fávero, L. Colpini, H. Bernabe, M. Baesso, S. Specchia, O. Santos, Photocatalytic reduction of Hg (II) on TiO_2 and Ag/TiO_2 prepared by the sol–gel and impregnation methods, Desalination 270 (2011) 241–247, https://doi.org/10.1016/j.desal.2010.11.051.

[27] C. Xia, C. Liu, Z. Liu, D. Wu, Photocatalytic removal of toxic Hg(II) ions using TiO_2-modified bamboo charcoal as photocatalyst, Adv. Mater. Res 550−553 (2012) 2182–2185. Online: 2012−07−26.

[28] F.S. Zhang, J.O. Nriagu, H. Itoh, Photocatalytic removal and recovery of mercury from water using TiO_2-modified sewage sludge carbon, J. Photochem. Photobiol. A: Chem. 167 (2004) 223–228, https://doi.org/10.1016/j.jphotochem.2004.06.001, 167.

[29] N. Serpone, Y.K. Ah-You, T.P. Tran, R. Harris, R, E. Pelizzetti, H. Hidaka, AM1 Simulated Sunlight Photoreduction and Elimination of Hg(II) and CH3Hg(II) chloride salts from Aqueous Suspensions of Titanium Dioxide, Sol. Energy 39 (1987) 491–498, https://doi.org/10.1016/0038-092X(87)90056-9.

[30] G. Custo, M.I. Litter, D. Rodríguez, C. Vázquez, Total reflection X-ray fluorescence trace mercury determination by trapping complexation: application in advanced oxidation technologies, Spectrochimica Acta Part B 61 (2006) 1119–1123, https://doi.org/10.1016/j.sab.2006.05.012.

[31] J.M. Herrmann, J. Disdier, P. Pichat, Photocatalytic deposition of silver on powder titania: consequences for the recovery of silver, J. Catal. 113 (1988) 72–81, https://doi.org/10.1016/0021-9517(88)90238-2.

[32] K. Tanaka, K. Harada, S. Murata, Photocatalytic deposition of metal ions onto TiO_2 powder, Sol. Energy 36 (1986) 159–161, https://doi.org/10.1016/0038-092X(86)90121-0.

[33] M.R. Prairie, L.R. Evans, B.M. Stange, S.L. Martinez, An investigation of TiO_2 photocatalysis for the treatment of water contaminated with metals and organic chemicals, Environ. Sci. Technol. 27 (1993) 1776–1782, https://doi.org/10.1021/es00046a003.

[34] C. Miranda, J. Yáñez, D. Contreras, D.R. Garcia, W.F. Jardim, H.D. Mansilla, Photocatalytic removal of methylmercury assisted by UV-irradiation, Appl. Catal. B 90 (2009) 115–119, https://doi.org/10.1016/j.apcatb.2009.02.023.

[35] K. Tennakone, U.S. Ketipearachchi, Photocatalytic method for removal of mercury from contaminated water, Appl. Catal. B 5 (1995) 343–349, https://doi.org/10.1016/0926-3373(94)00052-2.

[36] E.M. de la Fournière, A.G. Leyva, E.A. Gautier, M.I. Litter, Treatment of phenylmercury salts by heterogeneous photocatalysis over TiO_2, Chemosphere 69 (2007) 682–688, https://doi.org/10.1016/j.chemosphere.2007.05.042.

[37] C. Miranda, J. Yáñez, D. Contreras, R. Garcia, C. Zaror, H.D. Mansilla, Phenylmercury degradation by heterogeneous photocatalysis assisted by UV-A light, J. Environ. Sci. Health A 48 (2013) 1642–1648, https://doi.org/10.1080/10934529.2013.815453.

[38] E.M. de la Fournière, M.I. Litter, E.A. Gautier, Detection of mercury species by HPLC using 2-mercaptopropionic acid as complex agent, J. Arg. Chem. Soc. 100 (2013) 1–8. ISSN printed 1852-1428.

[39] O. Yepsen, D. Contreras, P. Santander, J. Yáñez, H.D. Mansilla, D. Amarasiriwardena, Photocatalytic degradation of thimerosal in human vaccine's residues and mercury speciation of degradation by-products, Microchem. J. 121 (2015) 41–47, https://doi.org/10.1016/j.microc.2015.02.001.

[40] J.M. Meichtry, C. Colbeau-Justin, G. Custo, M.I. Litter, TiO_2-photocatalytic transformation of Cr(VI) in the presence of EDTA: comparison of different commercial photocatalysts and studies by Time Resolved Microwave Conductivity, Appl. Catal. B: Environ. 144 (2014) 189–195.

[41] F.B. Martí, F.L. Conde, S.A. Jimeno, Química Analítica Cualitativa, Paraninfo, Madrid, 1994, p. 435.

[42] I.M. Kolthoff, E.B. Sandell, E.J. Meehan-Stanley Bruckenstein, Análisis Químico Cuantitativo, Nigar, Buenos Aires, 1969, p. 808.

[43] S.S. Zumdahl, Chemical Principles, 6th ed, Houghton Mifflin Company, 2009, p. A22.

[44] H.E. Byrne, D.W. Mazyck, Removal of trace level aqueous mercury by adsorption and photocatalysis on silica–titania composites, J. Hazard. Mater. 170 (2009) 915–919, https://doi.org/10.1016/j.jhazmat.2009.05.055.

[45] M.J. López-Muñoz, A. Arencibia, L. Cerro, R. Pascual, A. Melgar, Adsorption of Hg (II) from aqueous solutions using TiO_2 and titanate nanotube adsorbents, Appl. Surf. Sci. 367 (2016) 91–100, https://doi.org/10.1016/j.apsusc.2016.01.109.

[46] Z. Ghasemi, A. Seif, T.S. Ahmadi, B. Zargar, F. Rashidi, G.M. Rouzbahani, Thermodynamic and kinetic studies for the adsorption of Hg (II) by nano-TiO_2 from aqueous solution, Adv. Powder Technol. 23 (2012) 148–156, https://doi.org/10.1016/j.apt.2011.01.004.

[47] M.E. Mahmoud, G.M. Nabil, H. Abdel-Aal, N.A. Fekry, M.M. Osman, Imprinting "Nano-SiO_2-Crosslinked Chitosan-NanoTiO_2" polymeric nanocomposite for selective and instantaneous microwave-assisted sorption of Hg(II) and Cu(II), ACS Sustainable Chem. Eng. 6 (2018) 4564–4573, https://doi.org/10.1021/acssuschemeng.7b03215.

[48] C.A. Brebbia, Water Pollution XII., WIT Press, Southampton, UK, 2014, p. 229.

[49] NTP. National Toxicology Program, 1992, https://cameochemicals.noaa.gov/chemical/20388 (accessed 20/09/2018).

[50] J.M. Meichtry, N. Quici, G. Mailhot, M.I. Litter, Heterogeneous photocatalytic degradation of citric acid over TiO_2. I: mechanism of 3-oxoglutaric acid degradation, Appl. Catal. B 102 (2011) 454–463, https://doi.org/10.1016/j.apcatb.2010.12.026.

[51] A.V. Emeline, K. Ryabchuk, N. Serpone, Dogmas and Misconceptions in Heterogeneous Photocatalysis. Some Enlightened Reflections, J. Phys. Chem. B 109 (2005) 18515–18521, https://doi.org/10.1021/jp0523367.

[52] F.J. Montoya, J.A. Velásquez, P. Salvador, The direct–indirect kinetic model in photocatalysis: a reanalysis of phenol and formic acid degradation rate dependence on photon flow and concentration in TiO_2 aqueous dispersions, Appl. Catal. B 88 (2009) 50–58, https://doi.org/10.1016/j.apcatb.2008.09.035.

[53] L.B. Khalil, M.W. Rophael, W.E. Mourad, The removal of the toxic Hg(II) salts from water by photocatalysis, Appl. Catal. B 36 (2002) 125–130, https://doi.org/10.1016/S0926-3373(01)00285-5.

[54] B. Deng, A.T. Stone, Surface-catalyzed chromium(VI) reduction: the TiO_2−CrVI−Mandelic acid system, Environ. Sci. Technol. 30 (1996) 463–472, https://doi.org/10.1021/es950156c.

[55] F. Roncaroli, M.A. Blesa, Kinetics of adsorption of carboxylic acids onto titanium dioxide, Phys. Chem. Chem. Phys. 12 (2010) 9938–9944, https://doi.org/10.1039/c003086d.

[56] T.D. Waugh, H.F. Walton, J.A. Laswick, Ionization constants of some organomercuric hydroxides and halides, J. Phys. Chem. 59 (1955) 395–399, https://doi.org/10.1021/j150527a004.

[57] G. Limousin, J.-P. Gaudet, L. Charlet, S. Szenknect, V. Barthès, M. Krimissa, Sorption isotherms: a review on physical bases, modeling and measurement, Appl. Geochem. 22 (2007) 249–275, https://doi.org/10.1016/j.apgeochem.2006.09.010.

[58] Z. Ramezani, N. Pourmand, A. Behfar, A. Momeni, Removal and recovery of mercury from chlor-alkali petrochemical wastes using γ-Fe_2O_3 nanoparticles, Appl. Petrochem. Res. 6 (2016) 403–411, https://doi.org/10.1007/s13203-016-0168-8.

[59] M. Velicu, X. Fu, R.P.S. Suri, K. Woods, Use of adsorption process to remove organic mercury thimerosal from industrial process wastewater, J. Hazard. Mat. 148 (2007) 599–605, https://doi.org/10.1016/j.jhazmat.2007.03.015.

[60] C.H. Giles, T.H. MacEwan, S.N. Nakwa, S. Smith, Studies in Adsorption. Part XI. A System of Classification of solution adsorption isotherms and its use in diagnosis of adsorption mechanisms and in measure of specific surface area of solids, J. Chem. Soc. (1960) 3973–3993, https://doi.org/10.1039/jr9600003973.

[61] W. Liu, X. Zhao, T. Wang, J. Fu, J, Selective and irreversible adsorption of mercury (II) from aqueous solution by a flower-like titanate nanomaterial, J. Mater. Chem. A Mater. Energy Sustain. 3 (2015) 17676–17684, https://doi.org/10.1039/C5TA04521E.

[62] K.S.W. Sing, D.H. Everett, R.A.W. Haul, L. Moscon, R.A. Pierotti, J. Rouquerol, T. Siemieniewska, Reporting physisorption data for gas/solid systems with special reference to the determination of surface area and porosity, Pure Appl. Chem. 57 (4) (1985) 603–619, https://doi.org/10.1351/pac198557040603.

[63] M.I. Cabrera, O.M. Alfano, A.E. Cassano, Absorption and scattering coefficients of titanium dioxide particulate suspensions in water, J. Phys. Chem. 100 (1996) 20043–20050, https://doi.org/10.1021/jp962095q.

[64] A. Bakac, J.H. Espenson, Disproportionation and combination of ethyl radicals in aqueous solution, J. Phys. Chem. 90 (1986) 325–327, https://doi.org/10.1021/j100274a025.

[65] E. Baciocchi, M. Bietti, S. Steenken, Reactivity of $[CoIII\ W1_2O_{40}]^{5-}$ with organic radicals in aqueous solution. Evidence for an electron transfer mechanism, J. Chem. Soc. Perkin Trans. I 2 (1996) 1261–1263, https://doi.org/10.1039/p29960001261.

[66] N.S. Hush, K.B. Oldham, The electroreduction of organic iodides and organomercuric halides, J. Electroanal. Chem. 6 (1963) 34–45.

[67] H.H. Mohamed, N.A. Alomair, D.W. Bahnemann, Kinetic and mechanistic features on the reaction of stored TiO_2 electrons with Hg(II), Pb(II) and Ni(II) in aqueous suspension, Arab. J. Chem. 12 (2019) 5134–5141, https://doi.org/10.1016/j.arabjc.2016.08.001.

[68] J.M. Meichtry, R. Dillert, D. Bahnemann, M.I. Litter, Application of the stopped flow technique to the TiO_2-heterogeneous photocatalysis of hexavalent chromium in aqueous suspensions. Comparison with O_2 and H_2O_2 as electron acceptors, Langmuir 31 (2015) 6229–6236, https://doi.org/10.1021/acs.langmuir.5b00574.

[69] WHO (World Health Organization), Guidelines for Drinking-water Quality, 4rd ed., WHO (ed.), Geneva, Switzerland, 2011 (accessed 20/08/2018), http://whqlibdoc.who.int/publications/2011/9789241548151_eng.pdf.

[70] Código Alimentario Argentino (CAA), Artículos: 982 al 1079 - Bebidas Hídricas, Agua y Agua Gasificadas. (Res Conj. SPRYRS y SAGPYA N° 68/2007 y N° 196/2007)", 2012 (accessed 11/09/2018), http://www.anmat.gov.ar/alimentos/codigoa/CAPITULO_XII.pdf.

[71] F.A. Cotton, G. Wilkinson, Química Inorgánica Avanzada, Limusa, México, 1998, p. 715.

[72] D. Zhang, Y. Yin, Y. Li, Y. Cai, J. Liu, Critical role of natural organic matter in photodegradation of methylmercury in water: molecular weight and interactive effects with other environmental factors, Sci. Total Environ. 578 (2017) 535–541, https://doi.org/10.1016/j.scitotenv.2016.10.222.